Gaussian Process Latent Variable Alignment Learning (supplement)

Ieva Kazlauskaite
University of Bath, UK
Electronic Arts
i.kazlauskaite@bath.ac.uk

Carl Henrik Ek
University of Bristol, UK

Neill D. F. Campbell
University of Bath, UK
Royal Society
n.campbell@bath.ac.uk

1 Datasets with quantifiable comparisons

Fig. 1 and Fig. 2 give an example of the alignments and the warps produced by our method on the quantifiable dataset, see §4 in the paper. The detailed results of our experiments on this dataset are provided in Table 1.

2 Motion capture dataset

In this experiment we use the full set of joint motions to align a set of sports actions (see §4 for further information on the motion capture dataset). In Fig. 3 we provide an illustration of the power of using a generative model for alignment. New locations in the manifold encode novel motion sequences that are supported by the data. By allowing the model to align the data, it greatly improves the generative power as the model is capable of producing a wider range of plausible motions.

3 iPhone motion data

This dataset contains aerobic actions recorded using the Inertial Measurement Unit (IMU) on a smartphone [3], which contain high frequency variations. Unlike previous methods [4], which require the data to be smoothed first, our framework allows us to take into account the prior belief about the dataset in a principled way. By replacing the smooth RBF kernels for modeling the data with a Matérn $1/2$ kernel and taking into account the periodic nature of the actions by also including an additive periodic kernel, we are able to model the data without the need for preprocessing. Furthermore, by removing the smoothing prior from the warping functions, we allow the warps to be more flexible improving the alignment accuracy.

The alignment results for the iPhone motion data are shown in Fig. 4. The IMU includes a 3D accelerometer, a gyroscope, and a magnetometer, and records samples at 60 Hz. As in [4], for our experiment we take the accelerometer data in the x-direction for the jumping actions from subject 3, and, in particular, we look at 5 sequences each of which contains 400 frames. A Matérn $1/2$ kernel and a periodic kernel are used to fit the sequences as they contain high frequency variations, and we remove the smoothness constraint from the model of the warping functions to allow them to be more flexible.

4 Shift task

A common task in functional data alignment is that of estimating uniform translations of the time axis. One particular problem described by Marron *et al.* is that of aligning nuclear magnetic resonance (NMR) spectrum corresponding to different chemical components (e.g. ethanol) for a set of wines [2]. It is known that pH differences in wines induce a shift in values of the components and impedes their identification [1]. As shown by Marron *et al.* the alignment may be achieved using uniform shifts and minimizing the loss that requires sequences to be proportional to each other. Such operation is included in our model allowing us to perform the task of NMR spectrum alignment, and we are able to demonstrate a separation in the phase between the red wines and the white and rosé wines, see Fig. 5.

References

[1] F.H. Larsen, F. Van Den Berg, and S.B. Engelsen. An exploratory chemometric study of 1h nmr spectra of table wines. *Journal of Chemometrics*, 20(5), 2006.

[2] J.S. Marron, J.O. Ramsay, L.M. Sangalli, and A. Srivastava. Functional data analysis of amplitude and phase variation. *Statistical Science*, 30(4):468–484, 2015.

[3] Corey McCall, Kishore K. Reddy, and Mubarak Shah. Macro-class selection for hierarchical k-nn classification of inertial sensor data. In *PECCS*, 2012.

[4] J. D. Tucker, W. Wu, and A. Srivastava. Generative models for functional data using phase and amplitude separation. volume 61, pages 50–66, 2013.

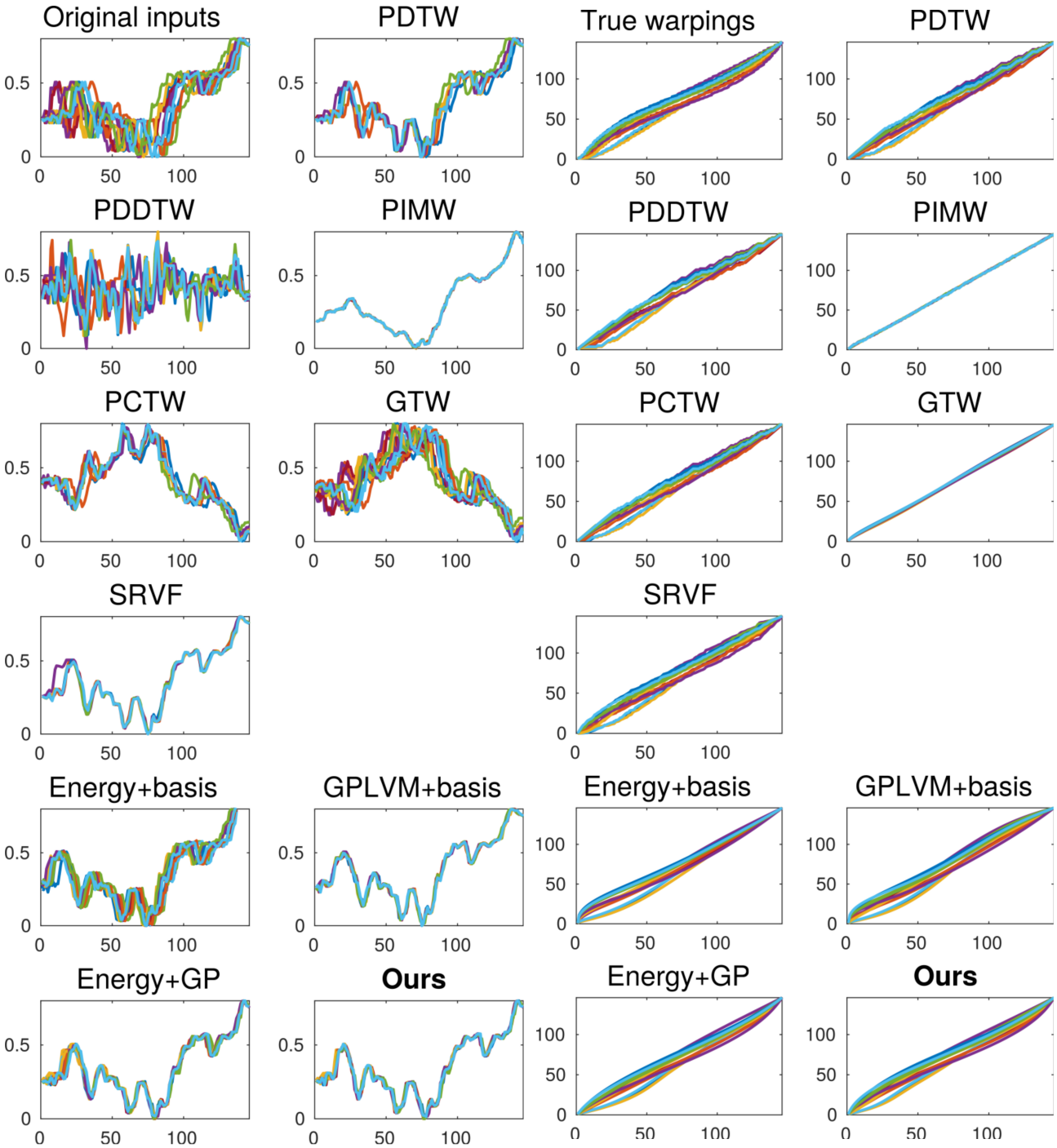

Figure 1: Original inputs and aligned sequences estimated by DTW, DDTW, IMW, CTW, GTW, SRVF, our approach and its three variants.

Figure 2: True warps and warps estimated by DTW, DDTW, IMW, CTW, GTW, SRVF, our approach and its three variants.

Dataset no	1	2	3	4	5	6	7	8	9	10	11	12	13	14	15	16	17	18	19	20	21	22	23	24	25	Mean
J	13	10	10	7	13	6	6	12	3	10	13	8	6	10	7	5	5	14	8	3	8	11	7	6	9	
T	258	157	107	246	169	131	92	144	138	298	146	240	204	213	157	230	247	196	248	277	141	153	83	285	178	
PDTW	9.32	14.38	5.88	12.42	10.57	10.03	2.30	6.60	2.41	16.99	9.84	13.47	4.95	16.72	4.00	6.97	14.03	6.57	15.01	1.98	4.44	5.16	5.05	13.19	10.85	8.93
PDDTW	10.55	14.67	6.80	13.86	12.18	10.30	2.58	7.35	3.95	24.59	10.68	15.45	6.57	18.60	5.54	8.35	14.91	7.70	16.38	5.37	6.11	7.43	5.44	14.02	11.17	10.42
PIMW	26.61	19.27	13.36	24.59	21.16	14.75	6.48	22.14	5.36	38.54	18.06	26.72	16.77	28.39	9.54	22.31	21.23	22.35	27.54	11.13	12.05	18.45	9.06	30.40	16.54	19.31
PCTW	12.12	15.30	9.50	18.89	15.45	11.32	2.77	10.58	2.66	17.26	9.98	24.72	8.04	17.19	6.23	10.21	16.03	10.73	15.17	7.12	5.88	5.59	6.00	16.92	10.98	11.47
GTW	6.52	9.54	6.54	6.96	7.50	3.23	4.27	10.63	0.86	33.31	2.55	21.28	5.35	4.72	3.38	23.28	8.50	10.70	2.83	3.93	2.74	2.56	5.45	15.70	2.63	8.20
SRVF	6.74	3.41	4.73	8.06	6.94	4.14	2.14	3.34	3.10	8.65	5.13	5.33	3.57	7.37	5.78	7.02	4.87	4.71	5.54	5.12	3.82	4.55	2.22	4.53	7.04	5.11
energy+basis	9.91	5.08	4.69	6.12	6.89	3.06	2.10	5.33	0.98	14.45	6.64	6.57	2.10	10.38	2.74	3.83	5.13	7.94	5.67	1.37	4.42	5.79	2.12	5.00	4.88	5.33
gplvm+basis	5.85	3.09	2.98	5.29	3.65	2.24	1.31	3.53	0.87	**1.85**	3.67	**3.68**	**1.49**	5.58	1.58	3.55	3.69	**2.13**	3.12	**1.22**	3.20	3.59	1.35	**1.72**	**1.90**	2.88
energy+gplvm	6.80	**2.45**	3.29	6.35	5.31	2.58	1.39	**3.23**	0.97	4.54	2.97	4.34	2.79	3.37	3.16	3.22	4.12	3.48	2.64	2.07	3.94	2.69	2.20	2.18	2.65	3.31
ours	**4.39**	4.55	**1.79**	**1.93**	**2.34**	**1.91**	**1.23**	4.68	**0.84**	3.49	**2.11**	4.94	3.47	**3.14**	**1.40**	**3.03**	**2.01**	2.57	**2.10**	1.48	**2.20**	**1.93**	**1.31**	2.87	2.11	**2.55**

Table 1: Datasets used for our evaluation where J and T refer to the number of sequences and dimensionality. Results are presented as MSE of warpings. The summary of the results presented in this table is given in Fig. 3 in the paper.

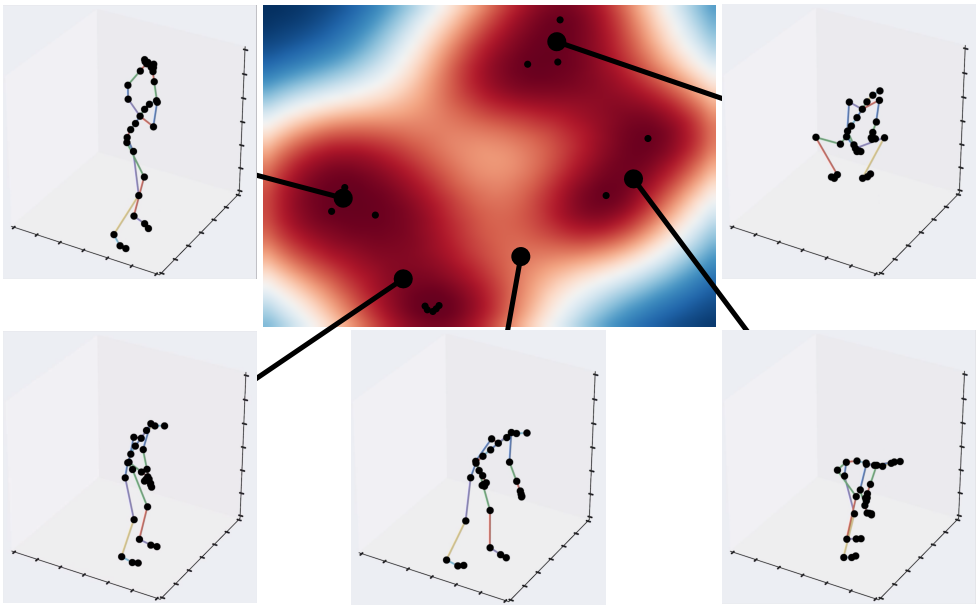

Figure 3: An advantage of our approach is that it not only aligns the data but is also a generative probabilistic model. Here we show novel sequences generated at new locations in the manifold. The black dots indicate the embedded locations of the training sequences. We note that, while we have only shown still images, each manifold location describes an entire time series. A video showing this is included with the supplementary material.

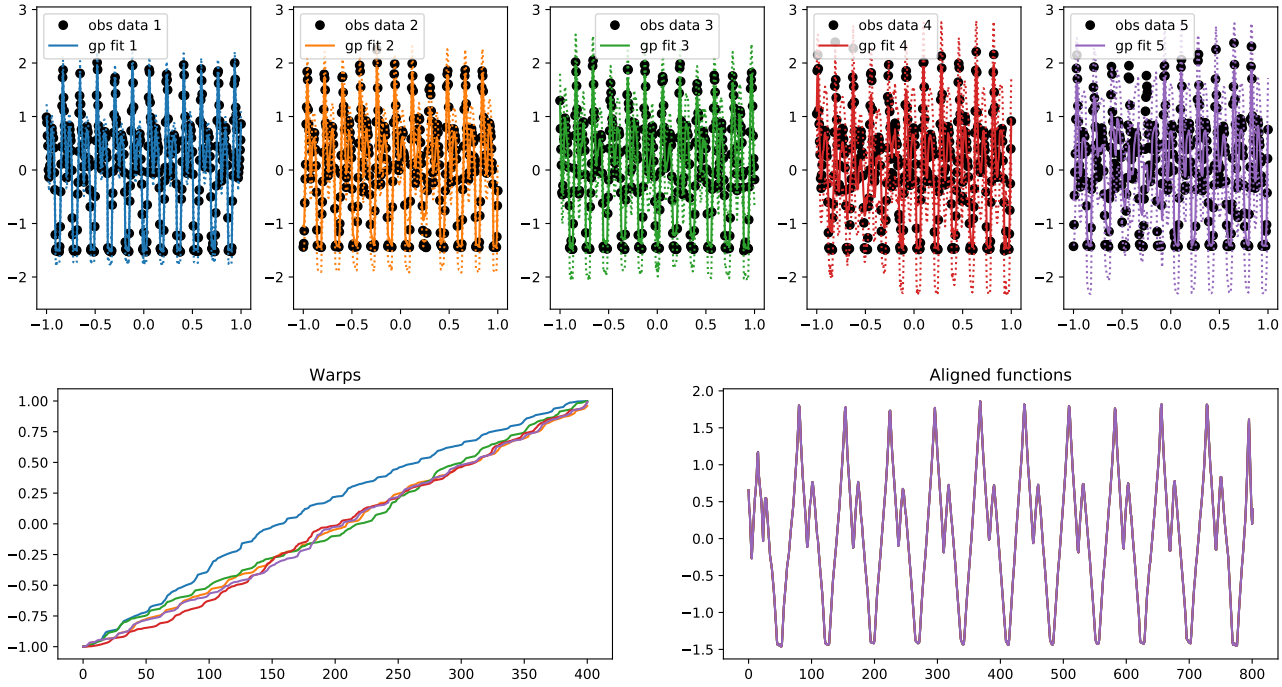

Figure 4: The top row shows the observed data and the fitted Gaussian Processes. The bottom row shows the corresponding warps (left) and the aligned functions.

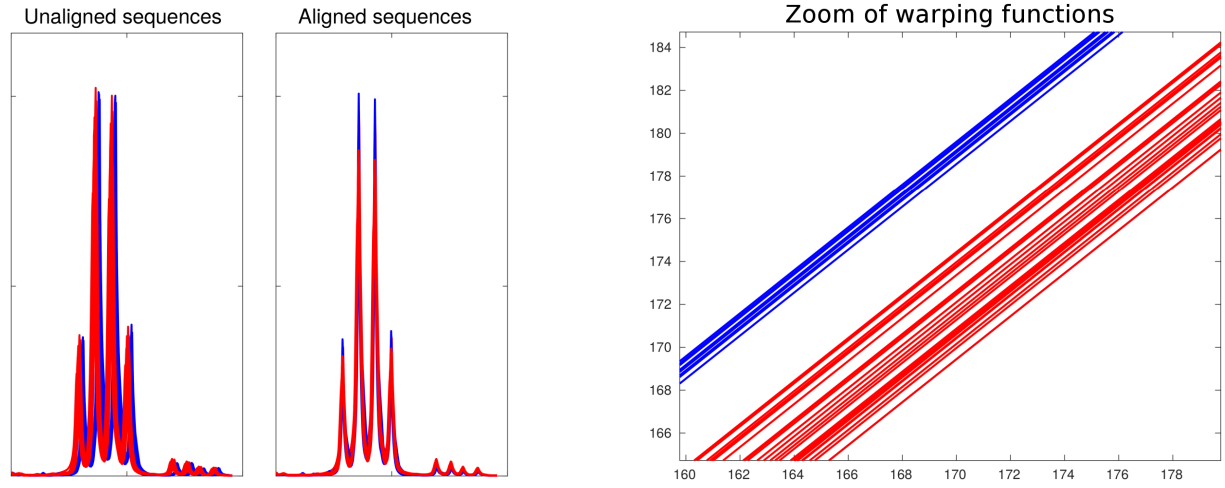

Figure 5: Alignment of NMR spectrum data [2]. The zoom of the warping functions show the separation of the white/rosé wines (shown in blue) and red wines (shown in red).